



HAL
open science

Localized states in bistable pattern forming systems

Umberto Bortolozzo, Marcel Clerc, Claudio Falcon, Stefania Residori, René Rojas

► **To cite this version:**

Umberto Bortolozzo, Marcel Clerc, Claudio Falcon, Stefania Residori, René Rojas. Localized states in bistable pattern forming systems. *Physical Review Letters*, 2006, 96, pp.214501. hal-00014398v2

HAL Id: hal-00014398

<https://hal.science/hal-00014398v2>

Submitted on 30 Jan 2006

HAL is a multi-disciplinary open access archive for the deposit and dissemination of scientific research documents, whether they are published or not. The documents may come from teaching and research institutions in France or abroad, or from public or private research centers.

L'archive ouverte pluridisciplinaire **HAL**, est destinée au dépôt et à la diffusion de documents scientifiques de niveau recherche, publiés ou non, émanant des établissements d'enseignement et de recherche français ou étrangers, des laboratoires publics ou privés.

Localized states in bistable pattern forming systems

U. Bortolozzo^{1,2}, M. G. Clerc³, C. Falcon³, S. Residori¹, and R. Rojas¹

¹*Institut Non Linéaire de Nice, UMR 6618 CNRS-UNSA,
1361Route des Lucioles, F-06560 Valbonne, France.*

²*Istituto Nazionale di Ottica Applicata, Largo E. Fermi 6 50125 Florence, Italy*

³*Departamento de Física, Facultad de Ciencias Físicas y Matemáticas,
Universidad de Chile, Casilla 487-3, Santiago, Chile.*

We present an unifying description close to a spatial bifurcation of localized states, appearing as large amplitude peaks nucleating over a pattern of lower amplitude. Localized states are pinned over a lattice spontaneously generated by the system itself. We show that the phenomenon is generic and requires only the coexistence of two spatially periodic states. At the onset of the spatial bifurcation, a forced amplitude equation is derived for the critical modes, which accounts for the appearance of localized peaks.

During the last years emerging localized structures in dissipative systems have been observed in different fields, such as domains in magnetic materials [1], chiral bubbles in liquid crystals [2], current filaments in gas discharge experiments [3], spots in chemical reactions [4], localized 2D states in fluid surface waves [5], oscillons in granular media [6], isolated states in thermal convection [7], solitary waves in nonlinear optics [8], just to mention a few. In one-dimensional systems, localized patterns can be described as homoclinic orbits passing close to a spatially oscillatory state and converging to an homogeneous state [9, 10], whereas domains are seen as heteroclinic trajectories joining the fixed points of the corresponding dynamical system [11]. Recently, in a nematic liquid crystal light valve with optical feedback it has been found experimentally a different type of localized states, appearing as a large amplitude peaks nucleating over a lower amplitude pattern and therefore called *localized peaks* [12]. Similar observations have been reported in a Newtonian fluid when non linear surface waves are parametrically excited with two frequencies [13] and in numerical simulations of an atomic vapor with optical feedback [14]. Recently, longitudinal modes with localized peaks over a spatially modulated background have been shown in numerical simulations of Maxwell-Bloch equations for a semiconductor laser [15].

All these different types of localized states appear over a patterned background and thus constitute a different class of structures with respect to the ones appearing over an uniform background. The aim of this manuscript is to show that localized peaks are a generic class of localized states, appearing whenever a pattern forming system exhibits coexistence of two spatially periodic states. The mechanisms that originate this circumstances are more than a few, for instance, one can consider a multi-stable system, which shows two consecutive spatial bifurcations to different states when one parameter is changed. There is a large number of physical systems that display this kind of behavior, therefore there is a vast number of possible models. In order to derive an unifying and simple description of localized peaks, we develop a theoretical model for one-dimensional spatially extended systems close to a spatial bifurcation. The model, which shows co-

existence between different patterns and stable front solutions between them, is based on an amplitude equation that includes a spatial parametric forcing. This extension with respect to conventional amplitude equations, allows to describe localized patterns and to account for the main properties of these solutions. The model includes the interaction of the slowly varying envelope with the small scale of the underlying pattern solution [16], well-known as the non-adiabatic effect [17, 18].

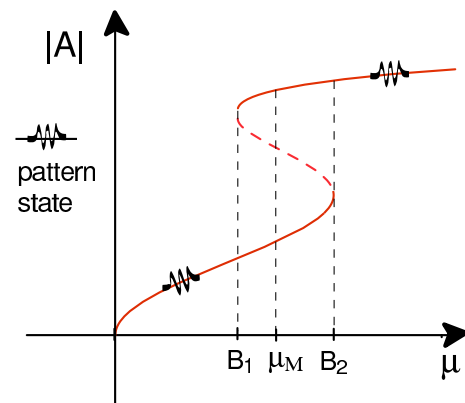


FIG. 1: A typical bifurcation diagram allowing for the appearance of localized peaks: at a certain value of μ a secondary subcritical bifurcation takes place; dashed lines mark the beginning (end) B_1 (B_2) of the bistable region and the Maxwell point μ_M .

Generally, the main ingredient for the appearance of localized peaks is the coexistence between two spatially periodic states. In order to give a generic description of such a situation, we consider a system that exhibits a sequence of spatial bifurcations as shown in Fig.1, that is, the primary bifurcation is super-critical while the secondary one is of subcritical type. Let $\vec{u}(x; t)$ be a vector field that describes the system under study and satisfies the partial differential equation

$$\partial_t \vec{u} = \vec{f}(\vec{u}, \partial_x, \{\lambda_i\}), \quad (1)$$

where $\{\lambda_i\}$ is a set of parameters. For a critical value of one of the parameters, the system exhibits a spatial

instability at a given wave number q_c . Close to this spatial instability, we use the ansatz $\vec{u} = A(X, T)e^{iq_c x} \hat{u} + \bar{A}(X, T)e^{-iq_c x} \hat{\bar{u}} + \dots$ and the amplitude satisfies [9]

$$\partial_T A = \mu A - \nu |A|^2 A + \alpha |A|^4 A - |A|^6 A + \partial_{XX} A, \quad (2)$$

where μ is the bifurcation parameter and $\{\nu, \alpha\}$ control the type of the bifurcation (first or second order depending on the sign of these coefficients). Higher-order terms are ruled out by scaling analysis, since $\nu \sim \mu^{2/3}$, $\alpha \sim \mu^{1/3}$, $|A| \sim \mu^{1/6}$, $\partial_t \sim \mu$, $\partial_x \sim \mu^{1/2}$, and $\mu \ll 1$. Note that this approach is phase invariant ($A \rightarrow Ae^{i\varphi}$), but the initial system under study does not necessarily have this symmetry.

As depicted in Fig.1, for a given range of parameter values the system exhibits coexistence between two different spatially periodic states, each one corresponding to a homogeneous state for the amplitude equation. The coexistence region is for $B_1 < \mu < B_2$. The extended stationary solution of the amplitude equation Eq.(2), has the form ($\partial_t A = 0$)

$$A = R_o e^{i \frac{\varepsilon}{R_o^2} X},$$

where $\mu - \varepsilon^2/R_o^4 - \nu R_o^2 + \alpha R_o^4 - R_o^6 = 0$ and ε is an arbitrary constant related to the initial phase invariance. It is worth to note that in the case of positive ε , the wave number of the pattern is modified by the inverse of the square amplitude R_o^2 , so that patterns with larger amplitude have smaller wave number. At variance when ε is negative, the patterns with large amplitude have smaller wavelength. In Fig.2 are depicted two different patterns that coexist for the same parameters and the pattern with large amplitude has smaller wavelength, hence ε in this case is negative.

Note that the above amplitude equation is variational and can be written as

$$\partial_t A = - \frac{\delta \mathcal{F} [A, \bar{A}]}{\delta \bar{A}},$$

where

$$\mathcal{F} = - \int \left(\mu |A|^2 - \nu \frac{|A|^4}{2} + \alpha \frac{|A|^6}{3} - \frac{|A|^8}{4} - |\partial_X A|^2 \right) dx.$$

For given values of the parameters, the two stable uniform stationary states of Eq.(2) have the same energy, that is, the system is at the *Maxwell point*. Where the front between the two states does not propagate, that is, the front is motionless [19]. By moving away from the Maxwell point, the front dynamics is usually characterized by the motion of the core of the front, which is defined as the front position with the largest slope. In order to have a localized solution, we consider the interaction of two of these motionless fronts close to the Maxwell point. As a consequence of the asymptotic behavior of the front at infinity, the front interaction is attractive, and has the form [20]

$$\dot{\Delta} = -ae^{-\lambda \Delta} + \delta, \quad (3)$$

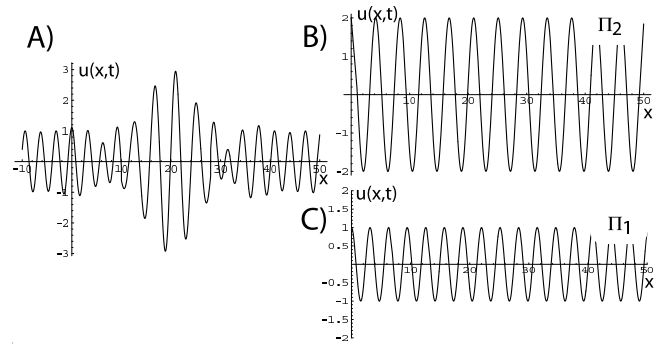


FIG. 2: Localized state and pattern solutions: a) localized state solution between pattern state Π_1 and Π_2 ; b) and c) represent the pattern solutions Π_1 and Π_2 coexisting for the same parameters.

where Δ is the distance between the cores of each front, δ is the separation from the Maxwell point ($\mu - \mu_M$), λ characterizes the exponential decay of the front to a given constant value at infinity, and a is a positive coefficient that characterizes the properties of the interaction and is determined by the form of the front. The Eq.(3) has an unstable fixed point $\Delta^* = -\ln(\delta/a)/\lambda$, which is the nucleation barrier between the two homogeneous states. Hence, the conventional amplitude equation, Eq.(2), does not exhibit stable localized states, due to the scale separation used to derive the amplitude equation. But near the front's core, the previous ansatz is no more valid. Indeed, in these locations the slowly varying envelope $A(X, T)$ shows oscillations of the same (or comparable) size as the small scale of the underlying pattern. This phenomenon is denominated as the non-adiabatic effect [17, 18].

In order to take into account this effect, we modify the amplitude equation by including the non-resonant terms. Thus, the amplitude equation becomes

$$\begin{aligned} \partial_T A = & \mu A - \nu |A|^2 A + \alpha |A|^4 A - |A|^6 A + \partial_{XX} A \\ & + \sum_{m,n \geq 0} g_{mn} A^m \bar{A}^n e^{-i \frac{q_c(1+n-m)}{\sqrt{\mu}} X} \end{aligned} \quad (4)$$

where g_{mn} are real numbers of order one. Now the amplitude equation is parametrically forced in space by the non-resonant terms. We note that the ansatz for \vec{u} satisfies the symmetries $\{x \rightarrow -x, A \rightarrow \bar{A}\}$, and $\{x \rightarrow x + x_o, A \rightarrow Ae^{iq_c x_o}\}$. Therefore, the envelope equation also is invariant under this transformation. Instead, the spatial translation and phase invariance are independent symmetries of Eq. (2).

To understand and illustrate the effect of non-resonant terms we keep the leading term $n = 0$ and $m = 2$. Then the amplitude equation takes the form

$$\begin{aligned} \partial_T A = & \mu A - \nu |A|^2 A + \alpha |A|^4 A - |A|^6 A + \partial_{XX} A \\ & + \eta A^2 e^{i \frac{q_c}{\sqrt{\mu}} X}. \end{aligned} \quad (5)$$

The amplitude is now spatially forced with frequency

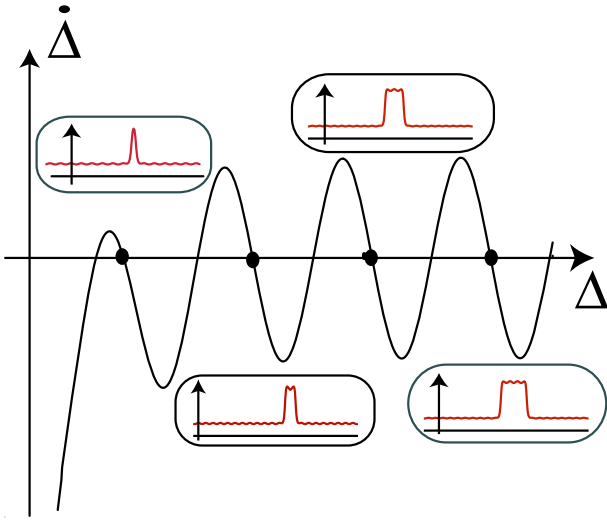


FIG. 3: Oscillatory interaction force between two front solutions. The inset figures are the stable localized patterns observed at the Maxwell points (black dots), where the interaction changes its sign.

$q_c/2\pi\sqrt{\mu}$ and amplitude $\eta \equiv g_{02}$. The spatial forcing is responsible for the homogenous states becoming a spatially periodic state. As a consequence, the front solution between the spatially periodic states exhibits a pinning range, that is, the front is motionless for a range of parameter around the Maxwell point. It is important to remark that the model (5) is the simplest model that exhibits front solution between two different spatial periodic solutions.

Note that the maxima of the envelope correspond to the maxima of the initial periodic solution $\bar{u}(t, x)$. In order to obtain the change of the front interaction as a result of the spatial forcing, we consider the front solution of the resonant equation

$A_{\pm}(x - x_o) = R_{\pm}(x - x_o)e^{i \int \varepsilon/R_{\pm}^2 dx}$, where $R_{\pm}(x - x_o)$ satisfies

$$\mu R - \nu R^3 + \alpha R^5 - R^7 + \partial_{xx} R - \frac{\varepsilon^2}{R^3} = 0,$$

x_o is the position of the front core and the lower index + (-) correspond to a front monotonically rising (decreasing). As the non resonant term is a rapid spatial oscillation, we consider this term as perturbative-type and use the ansatz

$$A = A_+(x - x_1(t)) + A_-(x - x_2(t)) - (A_{o,+} - A_{o,-}) + \delta W e^{i\delta\varphi},$$

in the Eq.(5), where $A_{o,\pm} = R_{o,\pm} e^{i\varepsilon x/R_{o,\pm}^2}$, and $\{\delta W, \delta\varphi\}$ are small functions, and $R_{o,\pm}$ are the stable equilibrium states of the resonant amplitude equation (2) and $R_{o,+} > R_{o,-}$. We obtain the following solvability condition for the δW function (front interaction)

$$\dot{\Delta} = -ae^{-\lambda\Delta} + \delta + \gamma \cos\left(\frac{q_c}{\sqrt{\mu}}\Delta\right), \quad (6)$$

with

$$a = \frac{-2\langle 3\mu R_+^2 - 5\nu R_+^4 + 7\alpha R_+^6 - 3\varepsilon R_+^{-4} | \partial_x R_+ \rangle}{\langle \partial_x R_+ | \partial_x R_+ \rangle},$$

$$\delta = \frac{F(R_+) - F(R_-)}{\langle \partial_x R_+ | \partial_x R_+ \rangle},$$

$$\gamma = \frac{\eta \langle \partial_x R_+ | R_+^2 \cos\left(\frac{q_c}{\sqrt{\mu}}x\right) \rangle}{\langle \partial_x R_+ | \partial_x R_+ \rangle},$$

$F(R) = \mu R^2/2 - \nu R^4/4 + \alpha R^6/6 - R^8/8 + 2\varepsilon^2/R^2$, and $\langle f|g \rangle \equiv \int_{-\infty}^{\infty} f(x)g(x)dx$.

As a consequence of the spatial forcing the interaction of two fronts close to the pinning range, Eq.(6), has an extra term and now alternates between attractive and repulsive forces. It is important to remark that γ is a parameter exponentially small, proportional to η , and is of order δ , i.e. the source of the *periodical force* is the spatial forcing in the Eq.(5). Therefore, close to the Maxwell point the system exhibits a family of equilibrium points, $d\Delta/dt = 0$. Each equilibrium point correspond to a localized solution nucleating over a pattern state, we call these solutions *localized patterns*. The lengths of localized patterns are multiple of a basic length, corresponding to the shortest localized state. We term these shortest states as *localized-peaks*, as these solutions correspond to the experimental observations reported in [12]. In Fig.3, it is depicted the front interaction and the family of equilibrium points.

Due to the oscillatory nature of the front interaction, which alternates between attractive and repulsive forces (cf. Fig.3), we can deduce the dynamical evolution and bifurcation diagram of localized patterns. By decreasing δ or increasing η , the family of localized patterns disappears by successive saddle-node bifurcations and only localized peaks survive. The mechanism for localized peak appearance is related to the fact that the spatial forcing is nonlinear. Indeed, it is proportional to the square of the pattern amplitude.

Since the amplitude of spatial forcing for the upper branch is larger than that for the lower branch, then the patterns with large modulus have large spatial amplitude oscillations around the equilibrium state of unperturbed amplitude equation (cf. Fig.(2)). Thus, for a given critical, and small, value of the forcing the pattern with high magnitude becomes unstable, because this state collides with the unstable pattern state. In Fig. (1), this unstable state is represented by the dashed line. Hence, the minima of the pattern with high magnitude reach the pattern with lower magnitude, and a saddle-node bifurcation of the spatial periodic solution gives rise to the appearance of a localized peak. Because of this mechanism, localized patterns with a size larger than the shortest length are not robust phenomena. In fact, the typical behavior observed in the experiments is the appearance of localized-peaks [12].

In Fig.4a, it is shown a localized peak profile recorded in the Liquid-Crystal-Light-Valve (LCLV) experiment

[12]. In order to directly compare with the model, we have performed one-dimensional experiments by inserting a rectangular slit in the optical feedback loop. The slit transverse size is approximately $100 \mu\text{m}$ whereas, for the parameters set in the experiment, the size of localized peaks is around $350 \mu\text{m}$. A similar profile can be numerically obtained for $\|\bar{u}\|^2 = |A|^2 \cos(q_c x)$, as shown in Fig.4b.

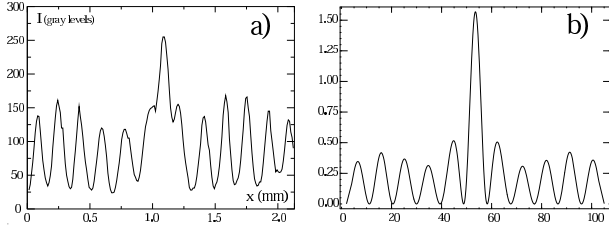


FIG. 4: a) Intensity profile of a one-dimensional localized peak in the LCLV experiment; b) $\|\bar{u}\|^2$ numerical profile in the presence of a localized peak.

In conclusion, we have presented an unifying description of localized peaks, which are large amplitude peaks nucleating over a lower amplitude pattern. We have derived a spatially forced amplitude equation and shown that localized peaks are a generic class of behavior appearing whenever a pattern forming system exhibits coexistence between two spatially periodic states. The front

solution that connects the two different pattern states exhibit a locking phenomena, that is, it is motionless for a range of parameter. We have obtained the front interaction and from this interaction we have deduced the family of localized solutions. We have shown that, as a consequence of the nonlinear nature of the forcing, localized patterns with a size larger than the shortest length are not robust phenomena, so that only localized peaks are stable at long times and for a wide range of parameters. We have shown a good qualitative agreement with the experimental observations for a LCLV system and we expect similar phenomena to be observed in other pattern forming systems, provided they present bistability between two different spatial structures. Note that pinning of localized structures on periodic arrays has recently been reported for a fixed grid [21]. Localized peaks can be seen as a generalization of this case, when the pinning lattice is spontaneously generated by the system itself.

The simulation software *DimX*, developed at INLN, has been used for all the numerical simulations presented in this paper. The authors thanks the support of ECOS-CONICYT collaboration program. M.G. C. acknowledges the financial support of FONDECYT project 1051117, and FONDAP grant 11980002. R.R. acknowledges financial support from Beca Presidente de la República of the Chilean Government.

-
- [1] H.A. Eschenfelder, *Magnetic Bubble Technology* (Springer Verlag, Berlin 1981).
- [2] S. Pirkel, P. Ribière and P. Oswald, *Liq. Cryst.* **13**, 413 (1993).
- [3] Y.A. Astrov and Y.A. Logvin, *Phys. Rev. Lett.* **79**, 2983 (1997).
- [4] K-Jin Lee, W. D. McCormick, J.E. Pearson and H.L. Swinney, *Nature* **369**, 215 (1994).
- [5] W.S. Edwards and S. Fauve, *J. Fluid Mech.* **278**, 123 (1994).
- [6] P.B. Umbanhowar, F. Melo and H.L. Swinney, *Nature* **382**, 793 (1996).
- [7] R. Heinrichs, G. Ahlers and D.S. Cannell, *Phys. Rev. A* **35**, R2761 (1987); P. Kolodner, D. Bensimon and C.M. Surko, *Phys. Rev. Lett.* **60**, 1723 (1988).
- [8] D.W. Mc Laughlin, J.V. Moloney and A.C. Newell, *Phys. Rev. Lett.* **51**, 75 (1983).
- [9] M. Cross and P. Hohenberg, *Rev. Mod. Phys.* **65**, 851 (1993).
- [10] P. Coulet, C. Riera and C. Tresser, *Phys. Rev. Lett.* **84**, 3069 (2000).
- [11] W. van Saarloos and P.C. Hohenberg, *Phys. Rev. Lett.* **64**, 749 (1990).
- [12] U. Bortolozzo, R. Rojas and S. Residori, *Phys. Rev. E* **72**, 045201(R) (2005).
- [13] H. Arbell and J. Fineberg, *Phys. Rev. Lett.* **85**, 756 (2000).
- [14] Yu. A. Logvin, B. Schäpers and T. Ackemann, *Phys. Rev. E* **61**, 4622 (2000).
- [15] L. Gil, private communication.
- [16] M.G. Clerc and C. Falcon, *Physica A* **356**, 48 (2005).
- [17] D. Bensimon, B.I. Shraiman, and V. Croquette, *Phys. Rev. A* **38**, R5461 (1988).
- [18] Y. Pomeau, *Physica D* **23**, 3 (1986).
- [19] P. Collet, J.P. Eckmann, *Instabilities and Fronts in Extended systems*, (Princeton University Press, New Jersey, 1990).
- [20] K. Kawasaki, and T. Ohta, *Physica A* **116**, 573 (1982).
- [21] T.J. Alexander, A. A. Sukhorukov, and Y. S. Kivshar, *Phys. Rev. Lett.* **93**, 063901 (2004).